# Non-Visual Light Sensing Enhances Behavioral Memory and Drives Gene Expression in *C. elegans*

Zhijian Ji[1, §], Bingying Wang[1, §], Rashmi Chandra[1, §], Junqiang Liu[1, §], Supeng Yang[1, 2], Yong Long[3], Michael Egan[1, 2], Noelle L'Etoile[4], Dengke K. Ma[1, 5, 6, *]

[1]Cardiovascular Research Institute, University of California San Francisco, San Francisco, CA 94158, USA.

[2]Department of Molecular Cell Biology, University of California, Berkeley, Berkeley, CA 94720, USA.

[3]Key Laboratory of Breeding Biotechnology and Sustainable Aquaculture, Institute of Hydrobiology, Chinese Academy of Sciences, Wuhan 430072, China.

[4]Department of Cell and Tissue Biology, University of California San Francisco, San Francisco, CA 94158, USA.

[5]Department of Physiology, University of California San Francisco, San Francisco, CA 94158, USA.

[6]Innovative Genomics Institute, University of California, Berkeley, Berkeley, CA 94720, USA.

[§] Equal contribution

*Correspondence: Dengke.Ma@ucsf.edu (D.K.M.)

## Abstract

Visible light influences a range of physiological processes, yet how animals respond to it independently of the visual system remains largely unknown. Here, we uncover a previously undescribed light-induced transcriptional pathway that modulates behavioral plasticity in *C. elegans*, a roundworm without eyes. We demonstrate that ambient visible light or controlled-intensity visible-spectrum LED activates an effector gene *cyp-14A5* in non-neuronal tissues through the bZIP transcription factors ZIP-2 and CEBP-2. Light induction of *cyp-14A5* is more prominent at shorter wavelengths but is independent of the known blue light receptors LITE-1 and GUR-3 in *C. elegans*. This bZIP-dependent genetic pathway in non-neuronal tissues enhances behavioral adaptability and olfactory memory, suggesting a body-brain communication axis. Furthermore, we use the light-responsive *cyp-14A5* promoter to drive ectopic gene expression, causing synthetic light-induced sleep and rapid aging phenotypes in *C. elegans*. These findings advance our understanding of light-responsive mechanisms outside the visual system and offer a new genetic tool for visible light-inducible gene expression in non-neuronal tissues.

## Introduction

Visible light is crucial for image formation and regulating various physiological processes through the visual system, yet how animals respond to ambient light independently of sight remains poorly understood. Recent studies have uncovered diverse non-visual photoreception mechanisms that modulate a range of biological processes, from circadian rhythms to stress responses and metabolic homeostasis[1–4]. These mechanisms often involve specialized light-sensitive proteins, such as opsins and cryptochromes, widely expressed in body locations, including the skin, brain, and peripheral organs. For example, mammalian melanopsin-expressing retinal ganglion cells play critical roles in systemic light responses largely independent of image formation[5–8]. In the nematode roundworm *C. elegans*, blue light photoreception requires the light-activated ion channels LITE-1 and GUR-3 in specific neurons, influencing aversive behaviors and cellular physiology[9–13]. Visible light irradiation can also cause photo-oxidative reactive oxygen species in animals[14–16]. Despite these advances, the molecular pathways and physiological outcomes of non-visual light sensing and responses remain largely unexplored, raising intriguing questions about the mechanistic basis and functional implications of light as an environmental cue beyond vision.

We previously studied how genes encoding cytochrome P450 (CYP) proteins respond to and mediate effects of exposure to environmental stresses in *C. elegans*[17,18]. Among various transcriptional reporters we generated for CYP-encoding genes to monitor environmental regulation, we serendipitously discovered that the *cyp-14A5* promoter-driven GFP expression is particularly sensitive to ambient visible light exposure. Building upon this initial finding, we conducted transcriptome profiling studies to identify

64 light-inducible genes in addition to *cyp-14A5*, determine key transcriptional regulators of
65 *cyp-14A5*, and show that the light-inducible CYP-14A5 promotes behavioral plasticity
66 and olfactory memory in *C. elegans*. The findings also provide a genetic tool to use
67 light-inducible *cyp-14A5* promoter to flexibly and ectopically drive gene expression.

68

69 **Results**

70 **Light activates expression of *cyp-14A5* and other genes in *C. elegans***

71 Cytochrome P450 proteins comprise a highly conserved superfamily of heme-containing
72 monooxygenases critical for metabolizing endogenous and xenobiotic compounds[19].
73 We constructed transcriptional reporters for genes encoding CYP in *C. elegans* and
74 found that *cyp-14A5p::GFP* was drastically up-regulated by bright-field transmission
75 light from a microscope inadvertently left on overnight. Using controlled light versus dark
76 conditions, we confirmed the finding from an integrated *cyp-14A5p::GFP* reporter and
77 observed its robust widespread GFP expression in many tissues induced by moderate-
78 intensity (500-3000 Lux, 16-48 hr duration) LED light exposure (**Fig. 1A**). The level of
79 GFP expression increased proportionally with both light intensity and duration, the
80 condition of which does not impact ambient temperature (**Fig. S1**), indicating that *cyp-*
81 *14A5p::GFP* expression is finely tuned to ambient light conditions (**Fig. 1B**).

82 To determine CYP-14A5 protein expression pattern, we constructed a translational GFP
83 (*cyp-14A5p::cyp-14A5::GFP*) reporter and observed robust light-induced expression of
84 CYP-14A5::GFP in many of the non-neuronal tissues, including the pharynx, hypoderm

85 and intestine (**Fig. 1C**). The transcriptional reporter exhibited similar patterns of non-
86 neuronal GFP induction by light (**Fig. 1A**). The translational reporter reveals CYP-
87 14A5::GFP patterns indicative of the endoplasmic reticulum structure (**Fig. 1C**),
88 consistent with the known subcellular localization of most CYPs to ER membranes[20].

89 To explore how eyeless *C. elegans* responds to ambient visible light independently of a
90 visual system, we conducted transcriptomic profiling by RNA-seq in *C. elegans* exposed
91 to controlled light or dark conditions. We found that defined light exposure (1500 Lux, 24
92 hr duration) to a synchronized population of young adults (24 hrs post L4) triggered a
93 robust genome-wide transcriptional response, including 7902 genes differentially
94 regulated (adjusted $P$ value < 0.05, **Fig. 1D** and **Table S1**). Among these, *cyp-14A5*
95 was one of the most strongly upregulated genes (**Fig. 1E**). Gene ontology (GO) analysis
96 of the light-induced transcriptome reveals their significant enrichment in several
97 pathways, including transmembrane signaling, pathogen and stress responses, protein
98 phosphorylation, cellular homeostasis and metabolisms (**Fig. S2**).

99 **ZIP-2 and CEBP-2 mediate light-induced transcriptional responses**

100 We next investigated the molecular regulators driving *cyp-14A5* activation in response
101 to light. To test if it requires previously identified blue-light receptors LITE-1 or GUR-3,
102 we crossed the *cyp-14A5p::GFP* reporter with *lite-1* and *gur-3* double loss-of-function
103 mutants. Interestingly, light-induced GFP expression was preserved in *lite-1gur-3*
104 double mutants, indicating that *cyp-14A5* activation operates through an alternative,
105 non-visual light-sensing mechanism (**Fig. 2A**). Prolonged photon exposure may also
106 cause photo-oxidation of DNA and genotoxicity, leading to DNA damage and ATM

107 protein-dependent check points and transcriptional responses[15,21,22]. However, loss of
108 the DNA damage sensor ATM-1 did not apparently affect light-induced GFP expression
109 (**Fig. 2A**). These findings underscore the existence of a novel light-responsive pathway
110 in *C. elegans*, distinct from previously characterized photoreceptive systems.

111 To identify transcriptional regulators driving *cyp-14A5* activation in response to light, we
112 adopted an RNAi-based screening strategy, focusing on approximately 400 genes
113 encoding transcription factors, including those responding to various types of stresses.
114 Knockdown of the expression of genes encoding TF from a previously assembled RNAi
115 library or selected for mediating various common stress responses (hypoxia, oxidative
116 stress, heat shock etc.) did not appear to affect *cyp-14A5* activation in response to light
117 (**Fig. 2B**). Surprisingly, we identified from such screen two pathogen-responding bZIP
118 transcription factors, ZIP-2 and CEBP-2, as critical mediators of light-induced *cyp-14A5*
119 transcription (**Fig. 2B**). Knockdown or genetic ablation of either *zip-2* or *cebp-2*
120 abolished light-induced *cyp-14A5p::GFP* expression (**Fig. 2B, 2C**). ZIP-2 and CEBP-2
121 have been previously identified[23–25] to cooperate in a regulatory complex and mediate
122 transcriptional responses to the bacterial pathogen *Pseudomonas aeruginosa* PA14. In
123 these studies, the *irg-1*p::GFP transcriptional reporter has been shown to be robustly
124 activated by PA14 as a well-established target for ZIP-2 and CEBP-2. Interestingly, we
125 found *irg-1*p::GFP was not activated by the same light condition (1500 Lux, 24 hrs) that
126 reliably induced *cyp-14A5*p::GFP (**Fig. 2D**). Although ZIP-2 can be activated by
127 pathogen stresses through ribosomal inhibition[23–25], our results highlight the specific
128 roles of ZIP-2 in mediating light-induced *cyp-14A5* but not *irg-1* reporter expression,
129 suggesting the involvement of additional stress-specific factors in these processes.

130 We further explored conditions and mechanisms leading to light-induced *cyp-*
131 *14A5p::GFP*. To test potential effects of ultraviolet (UV) irradiation from our visible light
132 LED, we used a UV-masking shield to block UV irradiation. However, this did not affect
133 visible LED light-induced *cyp-14A5p::GFP* expression (**Fig. 2E**). In addition, we found
134 that the LED light exposure of equal intensities (1500 Lux, 24 hrs) but at different
135 wavelengths (red, green, blue) led to differential *cyp-14A5p::GFP* expression (**Fig. 2F,**
136 **2G**), indicating stronger effects of shorter wavelengths in the visible light spectrum. A
137 pseudo-open reading frame (uORF) in the 5' untranslated region (UTR) of *zip-2* mRNA
138 inhibits the ribosomal translation of the ZIP-2 main open reading frame (mORF) in the
139 context of PA14 pathogen exposure[25]. However, constitutive expression of *zip-2* uORF
140 by the *rpl-28* promoter did not affect light-induced *cyp-14A5p::GFP* (**Fig. 2H**).
141 Furthermore, a CRISPR phospho-site knock-in mutation of *eif-2alpha(S49A)* did not
142 affect global translation[26], yet abolished light-induced *cyp-14A5p::GFP* (**Fig. 2I**). As the
143 eukaryotic eIF2alpha complex facilitates translational switch from uORF to mORF upon
144 stress-induced ribosomal stall at uORF[27–29], these results suggest that it is the *zip-2*
145 uORF translational inhibition, not the uORF protein product function, that mediates
146 visible light-induced ZIP-2 activation and *cyp-14A5p::GFP* reporter expression (**Fig. 2J**).

147 **Light-induced CYP-14A5 enhances behavioral memory**

148 Although EIF-2alpha and ZIP-2/CEBP-2 functions appear essential for light-induced up-
149 regulation of *cyp-14A5*, the *zip-2, cebp-2* or *cyp-14A5* loss-of-function null mutants
150 show no apparent body-size, morphological, feeding, defecation or developmental
151 defects under dark or LED light treatment (1500 Lux for 16 or 24 hrs) conditions (**Fig.**

152 **S3**). These data suggest that transient visible light exposure or light-induced *cyp-14A5*
153 activation by ZIP-2 does not broadly affect development or physiology, unlike long-term
154 visible light exposure, which has been shown to shorten lifespan in *C. elegans*[15].

155 The lack of obvious morphological and basal behavioral defects led us to explore
156 whether light exposure influences other aspects of *C. elegans* biology, particularly
157 behavioral plasticity and associative memory formation that might require integration of
158 body physiology. Specifically, we chose a learning paradigm in which animals learn to
159 avoid an innately attractive odor after it is paired with starvation[30,31]. They can
160 consolidate this learning into a long-lasting memory if the training is followed by sleep
161 within two hours[30]. Using this conditioning protocol (**Fig. 3A**), in which *C. elegans* learns
162 to avoid butanone (an innately attractive odor associated with nutritious bacteria) and
163 maintain the memory for up to 16 hours[30,31], we observed that animals exposed to
164 ambient light (approximately 500–1000 Lux) during olfactory associative learning and
165 recovery exhibited significantly enhanced memory retention compared to those
166 maintained in darkness (**Fig. 3B**). To pinpoint the critical period for light exposure, we
167 deprived animals of light in two-hour intervals immediately post-learning. Remarkably,
168 light deprivation during the first 2–4 hours post-learning resulted in markedly impaired
169 memory retention (**Fig. 3C**). These results suggest that environmental light exposure
170 enhances aversive cue association post learning and is not required for learning itself
171 but is required immediately post learning for consolidation of memory.

172 Does the light-modulated behavioral memory consolidation require light activation of the
173 ZIP-2 pathway? To address this question, we examined the behavioral memory of two

174 independent *zip-2* deletion mutants as compared to wild type (*cebp-2* mutants are
175 pleiotropically sick and thus not included). We found that both the *ok3730* and *tm4246*
176 deletion mutations of *zip-2* caused a significantly impaired memory consolidation but not
177 learning (**Fig. 3D**). Strikingly, the loss-of-function mutation of *cyp-14A5*, but not *F43C1.7*
178 (another ZIP-2 target gene induced by visible light), also impaired memory as *zip-2* (**Fig.**
179 **3E**), indicating a crucial role of the ZIP-2/CYP-14A5 regulatory axis in mediating light-
180 modulated memory consolidation. To further delineate the role of CYP-14A5, we
181 performed tissue-specific rescue experiments in the behavioral memory assay.
182 Hypoderm-specific expression of *cyp-14A5* restored the behavioral memory in the *cyp-*
183 *14A5* mutant (**Fig. 3F**). We observed similar degrees of rescue by two independently
184 derived lines expressing hypoderm-specific *dpy-7p::cyp-14A5* transgenes. These
185 findings strongly suggest that hypodermal induction of CYP-14A5 by ZIP-2 plays a
186 central role in mediating light-modulated behavioral memory.

187 **The *cyp-14A5* promoter as a versatile tool for light-inducible gene expression**

188 The light-responsive nature of the *cyp-14A5* promoter prompted us to explore its
189 potential as a tool for controlling gene expression. We generated synthetic constructs
190 driving the expression of diverse effectors under the *cyp-14A5* promoter to confer
191 striking organismal phenotypes. We previously found that *zip-10* expression promotes
192 organismal phenoptosis[32,33]. Driven by the *cyp-14A5* promoter, light-induced *zip-10*
193 expression indeed caused a robust light-dependent rapid aging or phenoptosis-like
194 phenotype with markedly shortened median and maximal lifespans (**Fig. 4A-4D**). We
195 confirmed that LED light exposure successfully induced *zip-10* expression, as

196 evidenced by robust ZIP-10-tagging mCherry fluorescence in major non-neuronal
197 tissues of transgenic animals, only after light (1500 Lux, 24 hrs) exposure (**Fig. 4B**).

198 To test organismal behavioral outcomes, we expressed *nlp-22* under the *cyp-14A5*
199 promoter. *nlp-22* was previously identified as a sleep-promoting neuropeptide[34–36],
200 overexpression of which can cause drastic reduction of pumping and locomotion speed,
201 characteristic of sleep behaviors in *C. elegans*. We found that *cyp-14A5p::nlp-22* can
202 indeed trigger striking behavioral quiescence upon light exposure (1500 Lux, 24 hrs), as
203 quantified by pumping rates, bending frequencies and locomotion speed (**Fig. 4E-4G,**
204 **S4**). These proof-of-concept studies demonstrate that the *cyp-14A5* promoter enables
205 light-dependent ectopic induction of gene expression, offering a flexible tool for probing
206 gene function, studies of organismal biology and synthetic physiology applications.

207

208 **Discussion**

209 Our findings uncover a previously unknown light-induced transcriptional pathway in *C.*
210 *elegans* that operates independently of known visual light receptors. Our study also
211 establishes a functional link between ambient light and behavioral plasticity through a
212 ZIP-2/CYP regulatory axis. The discovery of this pathway and its organismal functions
213 opens exciting avenues for understanding body-brain communication and how
214 environmental cues such as light can shape physiological and behavioral processes.

215 The specificity of this pathway is particularly intriguing, as *cyp-14A5* is robustly induced
216 by light at wavelength and intensity that do not apparently alter ambient temperature

217 (**Fig. S1**). Previous studies identified *cyp-14A5* as one of many genes moderately
218 regulated by bacterial pathogens[37–39], yet the classic pathogen-inducible gene reporter
219 *irg-1p::GFP* was not activated by light. This specificity raises important questions about
220 how ZIP-2 and *cyp-14A5* are selectively activated by light. Given the crucial roles of
221 ZIP-2 and eIF2alpha we find for light-induced expression of *cyp-14A5* and the
222 established role of the uORF at the 5' untranslated region of *zip-2* RNA in ZIP-2
223 regulation[25], it is plausible that light may regulate ZIP-2 translation by *zip-2* RNA photo-
224 oxidation at specific sites, eIF2alpha phosphorylation and specialized ribosomal
225 signaling[40–42]. Further investigation into the upstream signaling events and the
226 molecular sensors linking light exposure to ZIP-2/CEBP-2 activation is warranted.

227 Our behavioral assays demonstrate that light exposure enhances olfactory associative
228 memory, providing direct evidence for the functional relevance of light-induced *cyp-*
229 *14A5* expression. Interestingly, light exposure appears to exert its effects during a
230 specific temporal window immediately following learning, suggesting that light-induced
231 transcriptional changes post learning play a key role in memory consolidation. The
232 discovery of *cyp-14A5* as a key effector in this pathway also provides new insights into
233 how non-neuronal tissues contribute to behavioral plasticity. Our findings suggest that
234 light-induced CYP-14A5 and CYP-dependent metabolic or signaling changes in the
235 hypoderm may communicate with the nervous system to influence behavioral memory.
236 This body-brain communication axis highlights the importance of systemic integration in
237 mediating complex physiological and behavioral responses to environmental cues[43–46].

238 Beyond its biological significance, the light-inducible *cyp-14A5* promoter offers a useful
239 new tool for gene expression studies in *C. elegans*. The ability to drive ectopic gene

expression in response to light provides a versatile system for temporally controlled genetic manipulations. Our demonstration of light-induced sleep and mortality phenotypes through ectopic gene expression illustrates the potential applications of this tool in studying diverse biological processes in synthetic biology and physiology. Previous studies have used heat shock or drug-inducible promoters for temporally controlled gene expression in *C. elegans*[47–49]. The light-inducible *cyp-14A5* promoter provides an alternative, simple-to-implement approach and might be particularly useful when the drug-inducible system is cumbersome, or heat shock effects are undesirable.

While our study uncovers a novel light-responding mechanism with functional consequences in *C. elegans*, several limitations exist. First, the precise molecular mechanism by which visible light activates ZIP-2 and/or CEBP-2 remains unclear, as does the upstream signaling cascade linking light exposure to transcriptional activation. Second, although we demonstrate a functional connection between light-induced *cyp-14A5* expression and behavioral outcomes, the exact molecular interplay between peripheral transcriptional changes and neural plasticity requires further exploration. Finally, while the *cyp-14A5* promoter serves as a useful genetic tool, it does not confer tissue specificity, and its ectopic effector expression requires control for light effects. These limitations provide fertile ground for future research to build upon our findings.

## Materials & Methods

### *C. elegans* strains

262 *C. elegans* strains were grown on nematode growth media (NGM) plates seeded with
263 *Escherichia coli* OP50 at 20 °C with laboratory standard procedures unless otherwise
264 specified. The N2 Bristol strain was used as the reference wild type[50]. Mutants and
265 integrated transgenes were back-crossed at least 5 times. Genotypes of strains used are
266 as follows: *dmaIs156 IV [cyp-14A5p:: cyp-14A5::GFP; unc-54p::mCherry]*, *agIs17 IV [irg-*
267 *1p::gfp]*, *dmaEx [dpy-7p::cyp-14A5; myo-2p::mCherry], dmaEx [cyp-14A5p::zip-*
268 *10::mCherry; myo-2p::mCherry], dmaEx [cyp-14A5p::nlp-22; myo-2p::mCherry], cebp-2*
269 *(tm5421) I, eif-2alpha(rog3) I, zip-2(tm4248) III, zip-2(ok3730) III, cyp-14A5(gk152) V*.

270 PCR fusion constructs were used to generate transgenes[51], using primer sequences:

271 DM1310_*cyp-14A5*Pro c5p TCAACCACATCTTCCGATCA;
272 DM1311_*cyp-14A5*Pro to GFP c3p
273 CGACCTGCAGGCATGCAAGCTgatctttgttggacagaatagtttt;
274 DM2857_*dpy-7*p to *cyp-14A5* codutr Forward TGTCTCTGACGCCTGTGAGT;
275 DM2858_*dpy-7*p to *cyp-14A5* codutr Reverse
276 GATAAAGCAACGATGAAAACGCTCATTTTGTTTTCACAGAGCGGTAGA;
277 DM2944_*zip-2*uORF to *rpl-28*p-GOI-mCherry-5utr fusion F
278 CATCATAAAATAATTTATTTCCAGGTAAAATGTATCACGCAAAGACAACCACCG;
279 DM2945_*zip-2*uORF to *rpl-28*p-GOI-mCherry-5utr fusion
280 catgttatcttcttcacccttttgaggagccAAGCTCCCGTGGGAAGCTTGTG;
281 DM2948_*zip-10* to *cyp-14A5*p-GOI-mCherry-5utr fusion F
282 aaaactattctgtccaacaaagatcaaaATGACAACAATGACTAATTCTCTTATTTC;
283 DM2949_*zip-10* to *cyp-14A5*p-GOI-mCherry-5utr fusion R
284 catgttatcttcttcacccttttgaggagccGGAATGGTTGATTTGATTATTGAGTTG

285 DM2952_*nlp-22*cod::3utr to *cyp-14A5*p-GOI fusion

286 aaaactattctgtccaacaaagatcaaaATGCGTTCCATAATCGTCTTCATCG;

287 DM2953_*nlp-22*cod::3utr to *cyp-14A5*p-GOI fusion R cggttccactttctcatgagt

288

289 **Fluorescence microscopy and imaging**

290 SPE confocal (Leica) and epifluorescence microscopes were used to capture
291 fluorescence images. Animals were randomly picked at the same stage and treated with
292 1 mM levamisole in M9 solution (31742-250MG, Sigma-Aldrich), aligned on a 2% agar
293 pad on a slide for imaging. Identical setting and conditions were used to compare
294 experimental groups with control. For quantification of GFP fluorescence, animals were
295 outlined and quantified by measuring gray values using the ImageJ software. The data
296 were plotted and analyzed by using GraphPad Prism10.

297 For light-induced reporter imaging, reporter animals (synchronized young adults, 24 hrs
298 post L4) were exposed to white light (1500 Lux for 16 or 24 hrs, by Viribright 12-Watt, 800
299 Lumen, LED Desk Lamp Dimmable Office Lamp). For blue, green (SPE confocal, Leica),
300 and red light (HQRP 660 nm 14w LED pure red) conditions, animals of the same stage
301 were exposed to the same intensities (1500 Lux, 16 or 24 hours). Control groups from the
302 same batch of animals were maintained in darkness by opaque shields. Light intensities
303 and temperature were quantitatively measured by digital light meters and thermometers.

304

305 **RNA sequencing**

306 A synchronized population of wild-type young adult (24 hrs post L4) animals were
307 exposed to LED light (1500 lux, 24 hr duration, Viribright 12-Watt, 800 Lumen, LED Desk
308 Lamp Dimmable Office Lamp). Control groups from the same batch of animals were
309 maintained in darkness by opaque light shields. Four independent biological replicates
310 were used for both light-treated and control groups. For sample collection, the animals
311 were washed down from NGM plates using M9 solution and bacteria-cleaned with M9
312 washing in centrifuge tubes, homogenized by tissue disruptors and subjected to RNA
313 extraction using the RNeasy Mini Kit from Qiagen. 1 mg total RNA from each sample was
314 used for sequencing library construction. The libraries were constructed and sequenced
315 for paired end 150 bp by DNBseq (Innomics). The cleaned RNAseq reads were mapped
316 to the genome sequence of *C. elegans* using hisat2 and the mapped reads were assigned
317 to the genes using featureCounts[52,53]. The abundance of genes was expressed as RPKM
318 (Reads per kilobase per million mapped reads) and identification of differentially
319 expressed genes was performed using the DESeq2 package[54].

320

321 ***C. elegans* behavioral assays**

322 The olfactory behavioral memory assay was as described previously with modification[30,31].
323 Briefly, one day old adult worms (24 hrs post L4) were washed with S basal buffer (0.1M
324 NaCl, 0.05M $K_3PO_4$, pH 6.0) off 10 cm NGM plates and into microfuge tubes, where they
325 were washed three times with S basal buffer. The animals were split in two groups; one
326 group was added to a microfuge tube of S basal and the other group was added to a
327 microfuge tube of 1:10,000 dilution of butanone in S basal. The microfuge tubes were
328 then rotated for 80 minutes. The odor training includes three 80-minute cycles of training

329 with odor, or a control buffer interspersed with two 30-minute periods of feeding with OP50
330 *E. coli* bacteria. For chemotaxis assay, 1 μL of (1 M) $NaN_3$ was pipetted onto the odor
331 and diluent spots in 10 cm plastic petri dishes. 1 μL of 200 proof ethanol was added to
332 the diluent spot and 1 μL of 1:1000 butanone was added to the odor spot, while S basal
333 or butanone-trained worms were dropped onto the middle of 10 cm plastic petri dishes.
334 The recovery period was either under darkness or ambient light (600 Lux) for 16 hrs or
335 were kept under darkness for 2 or 4 hrs periods followed by light exposure and
336 chemotaxis to assay behavioral memory.

337 For sleep analysis induced by *cyp-14A5p::nlp-22*, the bending angles, moving average
338 speed, and track length of *C. elegans* after 48 hours of exposure to either light or dark
339 conditions were analyzed using WormLab. In such experiment, a synchronized population
340 of young adult (24 hrs post L4) animals of indicated genotype or transgene expression
341 were used. After light exposure or control dark treatment, they were transferred to a fresh
342 NGM plate seeded with a small OP50 bacterial lawn and allowed to settle for at least ten
343 minutes to recover at room temperature. After the recovery period, a one-hour recording
344 session was conducted using WormLab. Bending angles were calculated as described in
345 the referenced method as a metric for sleep behaviors[30]. Moving average speed was
346 determined by tracking the displacement of the worms over time.

347

348 **Statistics**

349 Numerical data were analyzed using GraphPad Prism 10 Software (Graphpad, San
350 Diego, CA) and presented as means ± S.D. unless otherwise specified, with *P* values

351 calculated by unpaired two-tailed t-tests (comparisons between two groups), one-way
352 ANOVA (comparisons across more than two groups) and two-way ANOVA (interaction
353 between genotype and treatment), with post-hoc Tukey and Bonferroni's corrections.
354 The lifespan assay was plotted and quantified using Kaplan–Meier lifespan analysis,
355 and *P* values were calculated using the log-rank test.

356

357 **Acknowledgment**

358

359 Some strains were provided by the *Caenorhabditis* Genetics Center (CGC), which is
360 funded by the NIH Office of Research Infrastructure Programs (P40 OD010440), and by
361 Dr. E. Troemel. We also thank the *C. elegans* Reverse Genetics Core Facility
362 (University of British Columbia), National Bioresource Project (S. Mitani, Tokyo
363 Women's Medical University, Tokyo, Japan), Wormbase.org (NIH grant #U24
364 HG002223 to P. Sternberg), Wormatlas.org (NIH grant #OD010943 to D.H. Hall.), Aging
365 Atlas (Dr. M. Wang) and CenGen (cengen.org) for their immensely helpful resources.
366 The work was supported by NIH grants (R35GM139618 to D.K.M.), BARI Investigator
367 Award (D.K.M.), and UCSF PBBR New Frontier Research Award (D.K.M.)

368

369 **Author Contributions**

370

371 D.K.M. designed and analyzed the *C. elegans* experiments, contributed to project
372 conceptualization and wrote the manuscript. B.W. made the initial observation on *cyp*-

373 *14A5* induction by light and performed RNAi screens and reporter imaging. Z.J.
374 prepared RNA-seq samples and characterized light effects on the *cyp-14A5* reporter,
375 cellular, behavioral and physiological phenotypes of various mutants with assistance
376 from W.Y. and M.E. Y.L. analyzed the RNA-seq data. R.C. designed, performed and
377 analyzed the behavioral memory assays. J.L. designed, performed and analyzed the
378 light-induced sleep and phenoptotic aging assays. N.L., Y.L., B.W., Z.J., R.C., J.L.
379 contributed to research materials, project conceptualization and editing manuscript.
380
381
382 **Competing Interest Statement:** The authors declare no competing interests.
383
384
385

386 **Figures and figure legends**

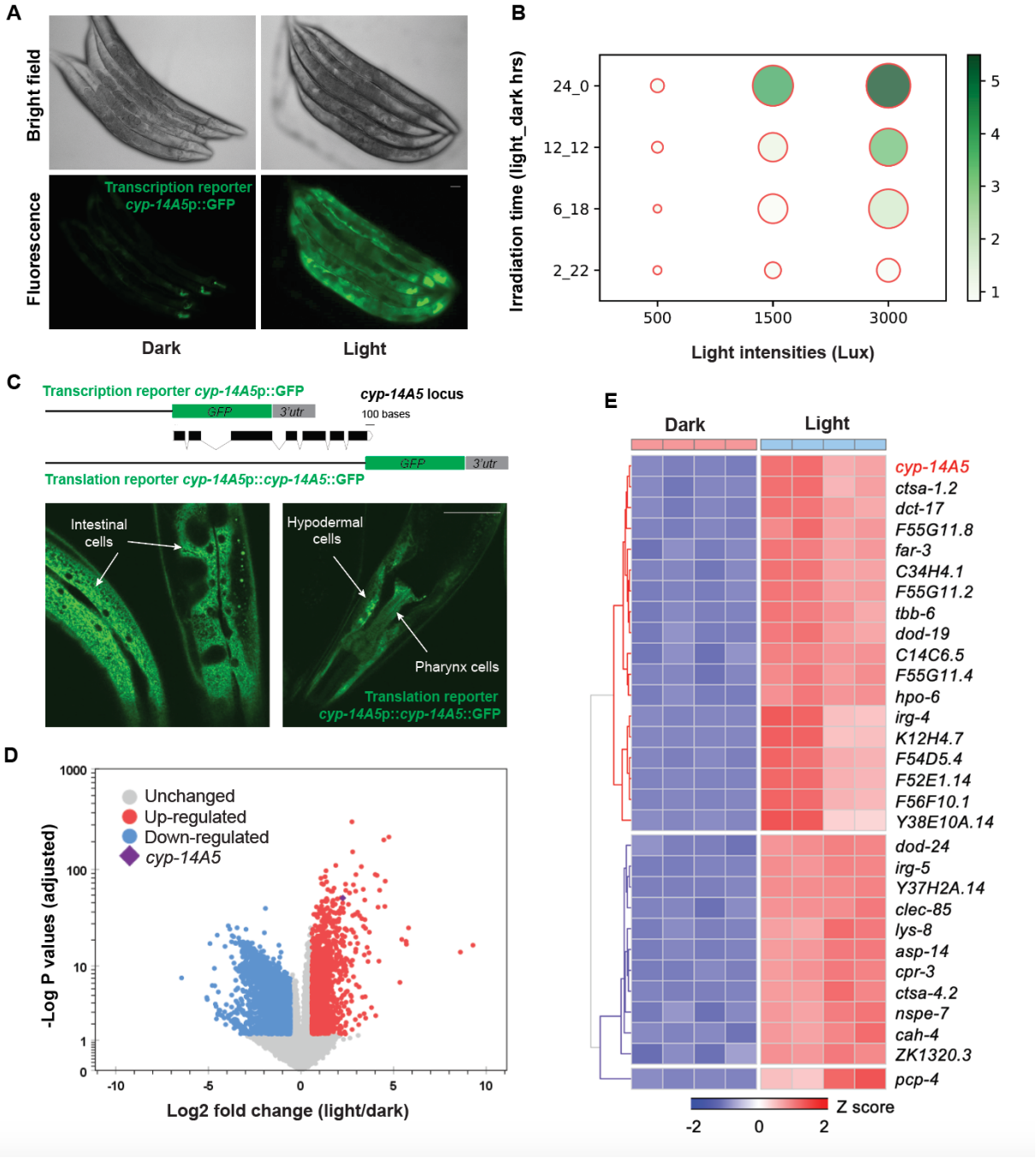


387

388 **Figure 1 Light exposure activates the CYP-encoding gene *cyp-14A5* in a genetic**

389 **program in *C. elegans***. A, Representative epifluorescence and brightfield images

390 showing *cyp-14A5*p::GFP induction by light exposure (1500 Lux, 24 hrs), in

synchronized young adults (24 hrs post L4). Scale bar: 50 µm. B, Dot plot showing fold induction of *cyp-14A5*p::GFP as a function of light intensity (Lux) and duration of light (hours of light_dark indicated in Y axis). C, Schematic of *cyp-14A5* transcriptional and translational GFP reporters. The translational reporter shows non-neuronal (major tissues indicated by arrows) induction of CYP-14A5::GFP by light (1500 Lux, 24 hrs). Scale bar: 50 µm. D, Volcano plot showing genes differentially regulated by light (1500 Lux, 24 hrs), with *cyp-14A5* highlighted, in synchronized young adults (24 hrs post L4). E, Heat map of top-ranking visible light-regulated genes (top 30 including *cyp-14A5*).

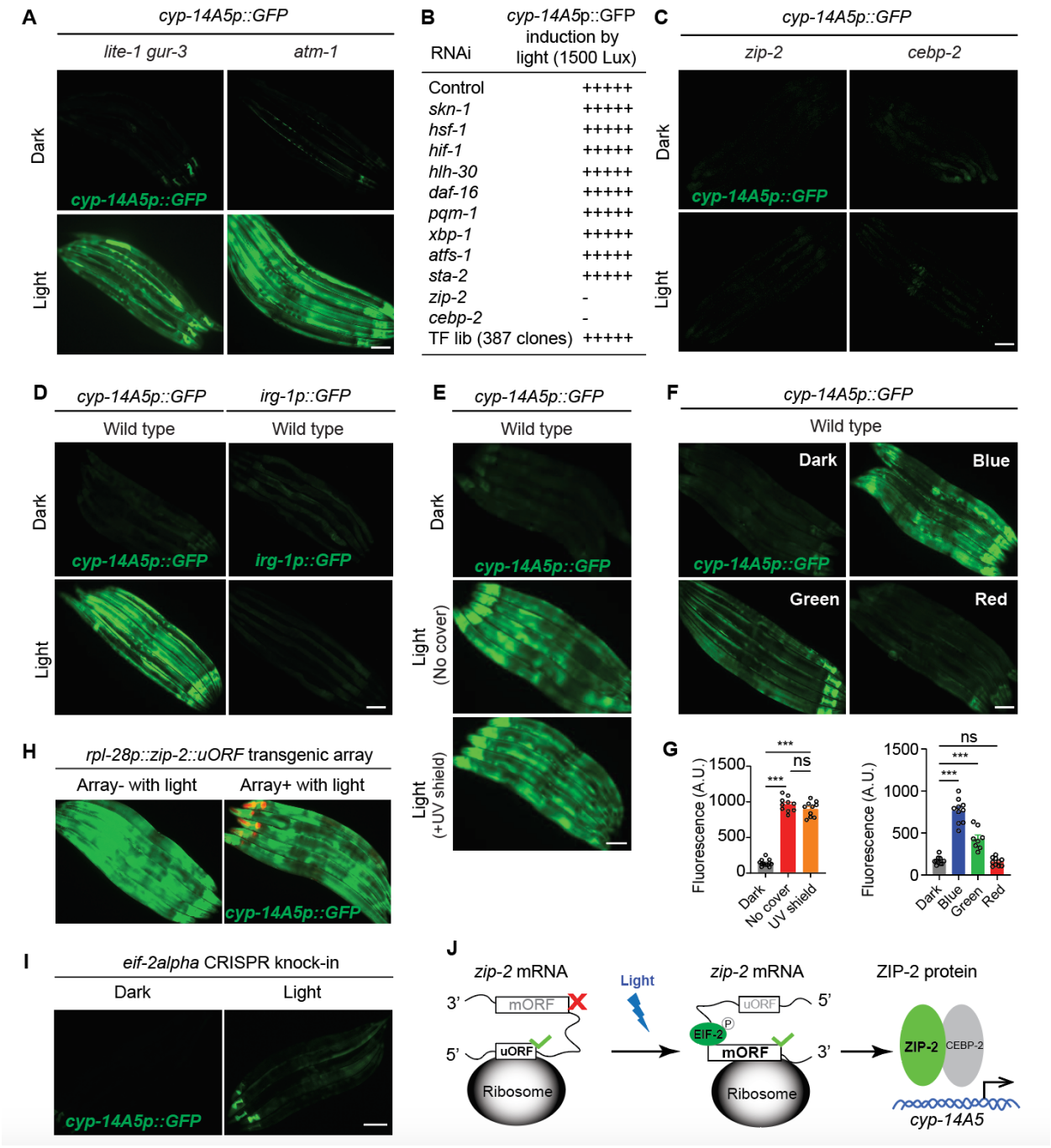


**Figure 2 Light induction of *cyp-14A5*p::GFP requires the transcription factors ZIP-2 and CEBP-2**. A, Representative epifluorescence images showing light-induced *cyp-14A5*p::GFP expression in *lite-1 gur-3* double and *atm-1* single loss-of-function mutants. Scale bar: 50 µm. B, Summary of RNAi screens identifying ZIP-2 and CEBP-2 as

405 essential transcriptional regulators of light-induced *cyp-14A5p::GFP* expression. C,
406 Representative epifluorescence images showing light-induced *cyp-14A5p::GFP*
407 expression in wild type, *zip-2* and *cebp-2* loss-of-function mutants. Scale bar: 50 μm. D,
408 Representative epifluorescence images showing light-induced *cyp-14A5p::GFP*
409 expression and no light-induced *irg-1p::GFP* expression in wild type animals. Scale bar:
410 50 μm. E, Representative epifluorescence images showing light-induced *cyp-*
411 *14A5p::GFP* expression unaffected by a UV shield. Scale bar: 50 μm. F, Representative
412 epifluorescence images showing light-induced *cyp-14A5p::GFP* expression by red,
413 green, blue LED light sources of equal intensities. Scale bar: 50 μm. G, Quantification of
414 E and F. *** indicates $P < 0.001$, n.s., non-significant. H, Representative
415 epifluorescence images showing light-induced *cyp-14A5p::GFP* expression unaffected
416 in *rpl-28p::zip-2uORF* transgenic animals. Scale bar: 50 μm. I, Representative
417 epifluorescence images showing light-induced *cyp-14A5p::GFP* expression abolished in
418 *eif-2alpha* mutants. Scale bar: 50 μm. J, Schematic model for light-induced transition of
419 *zip-2* mRNA from translating uORF to mORF, leading to increased ZIP-2 and
420 subsequent increased transcriptional *cyp-14A5* expression in cooperation with CEBP-2.
421 uORF and mORF are separated for clarity.

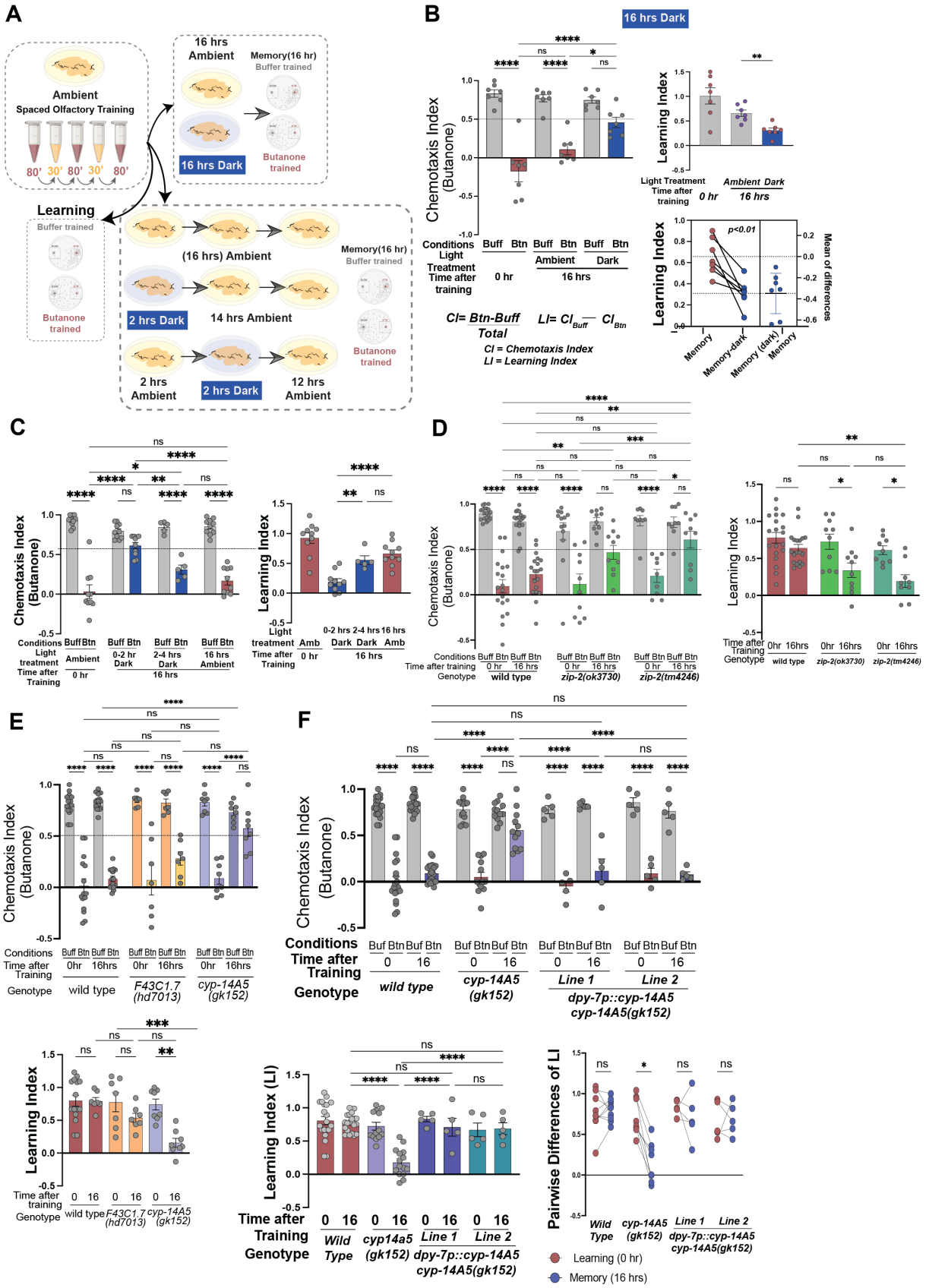
A
Ambient
Spaced Olfactory Training
80' 30' 80' 30' 80'
16 hrs Ambient
Memory(16 hr)
Buffer trained
16 hrs Dark
Butanone trained
Learning
Buffer trained
Butanone trained
(16 hrs) Ambient
Memory(16 hr)
Buffer trained
2 hrs Dark
14 hrs Ambient
Butanone trained
2 hrs Ambient
2 hrs Dark
12 hrs Ambient
B
16 hrs Dark
Chemotaxis Index (Butanone)
Conditions
Light Treatment
Time after training
Buff Btn Buff Btn Buff Btn
Ambient Dark
0 hr
16 hrs
CI= Btn-Buff / Total
LI= CI_Buff — CI_Btn
CI = Chemotaxis Index
LI = Learning Index
Learning Index
Light Treatment
Time after training
0 hr
Ambient Dark
16 hrs
p<0.01
Mean of differences
Memory
Memory-dark
Memory (dark)
Memory
C
Chemotaxis Index (Butanone)
Conditions
Light treatment
Time after Training
Buff Btn
Ambient
0 hr
0-2 hr Dark
2-4 hrs Dark
16 hrs Ambient
16 hrs
Learning Index
Light treatment
Time after Training
Amb
0 hr
0-2 hrs Dark
2-4 hrs Dark
16 hrs Amb
16 hrs
D
Chemotaxis Index (Butanone)
Conditions
Time after training
Genotype
Buff Btn
0 hr
16 hrs
wild type
zip-2(ok3730)
zip-2(tm4246)
Learning Index
Time after Training
Genotype
0hr 16hrs
wild type
zip-2(ok3730)
zip-2(tm4246)
E
Chemotaxis Index (Butanone)
Conditions
Time after Training
Genotype
Buff Btn
0hr 16hrs
wild type
F43C1.7 (hd7013)
cyp-14A5 (gk152)
F
Chemotaxis Index (Butanone)
Conditions
Time after Training
Genotype
Buf Btn
0 16
wild type
cyp-14A5 (gk152)
Line 1
Line 2
dpy-7p::cyp-14A5 cyp-14A5(gk152)
Learning Index
Time after training
Genotype
0 16
wild type
F43C1.7 (hd7013)
cyp-14A5 (gk152)
Learning Index (LI)
Time after Training
Genotype
0 16
Wild Type
cyp14a5 (gk152)
Line 1
Line 2
dpy-7p::cyp-14A5 cyp-14A5(gk152)
Pairwise Differences of LI
Wild Type
cyp-14A5 (gk152)
Line 1
Line 2
dpy-7p::cyp-14A5 cyp-14A5(gk152)
Learning (0 hr)
Memory (16 hrs)

423 **Figure 3 Light promotes sleep behavior and memory consolidation via a ZIP-**
424 **2/CYP axis from hypodermis**. A, Schematic of behavioral setup to test effects of dark
425 on olfactory memory. B, Wild-type learning and memory after 16 hours of dark
426 exposure. 7 trials, 50-200 animals per trial/condition. Two-way ANOVA shows
427 significant differences in chemotaxis (CI) under ambient light conditions (approximately
428 600 Lux) but not when the assay plates were placed in the dark. Learning (LI) indices
429 reflect the differences between buffer- and butanone-treated animals, abolished under
430 dark (one-way ANOVA). Pairwise t-tests of the amount of memory retention under light
431 and dark recovery reveal the degree of memory loss under dark. C, Dark exposure
432 timeline shows that exposing animals to dark immediately after training (0-2 hr, Dark)
433 shows hampered memory retention, whereas dark conditions for 2-4 hours period after
434 two hours after ambient light recovery is less sufficient to induce memory loss (two-way
435 ANOVA). The lack of differences between buffer and butanone-trained animals is
436 reflected in the respective LIs (one-way ANOVA). D, Two different loss-of-function
437 alleles of *zip-2(tm4246)* or *zip-2(ok3730)* both showed impaired memory, but learning
438 remained intact (two-way ANOVA). 5-10 trials, 50-200 animals per trial/condition. E,
439 Memory impairment of *cyp-14A5(gk152)* but not *F43C1.7* mutant animals (two-way
440 ANOVA for CIs and One-way ANOVA for LIs. 7-14 trials, 50-200 animals per
441 trial/condition. F, Memory defects of *cyp-14A5(gk152)* mutants are rescued by
442 hypodermal expression of wild-type *cyp-14A5*. Two independent transgenic lines show
443 similar results with comparison of pairwise differences in LIs and the amount of memory
444 rescued by hypodermal *cyp-14A5* (Cis: Two-way ANOVA; Lis: One-way ANOVA). *

445 indicates $P < 0.05$, ** indicates $P < 0.01$, *** indicates $P < 0.001$, **** indicates $P <$

446 $0.0001$, n.s., non-significant.

447

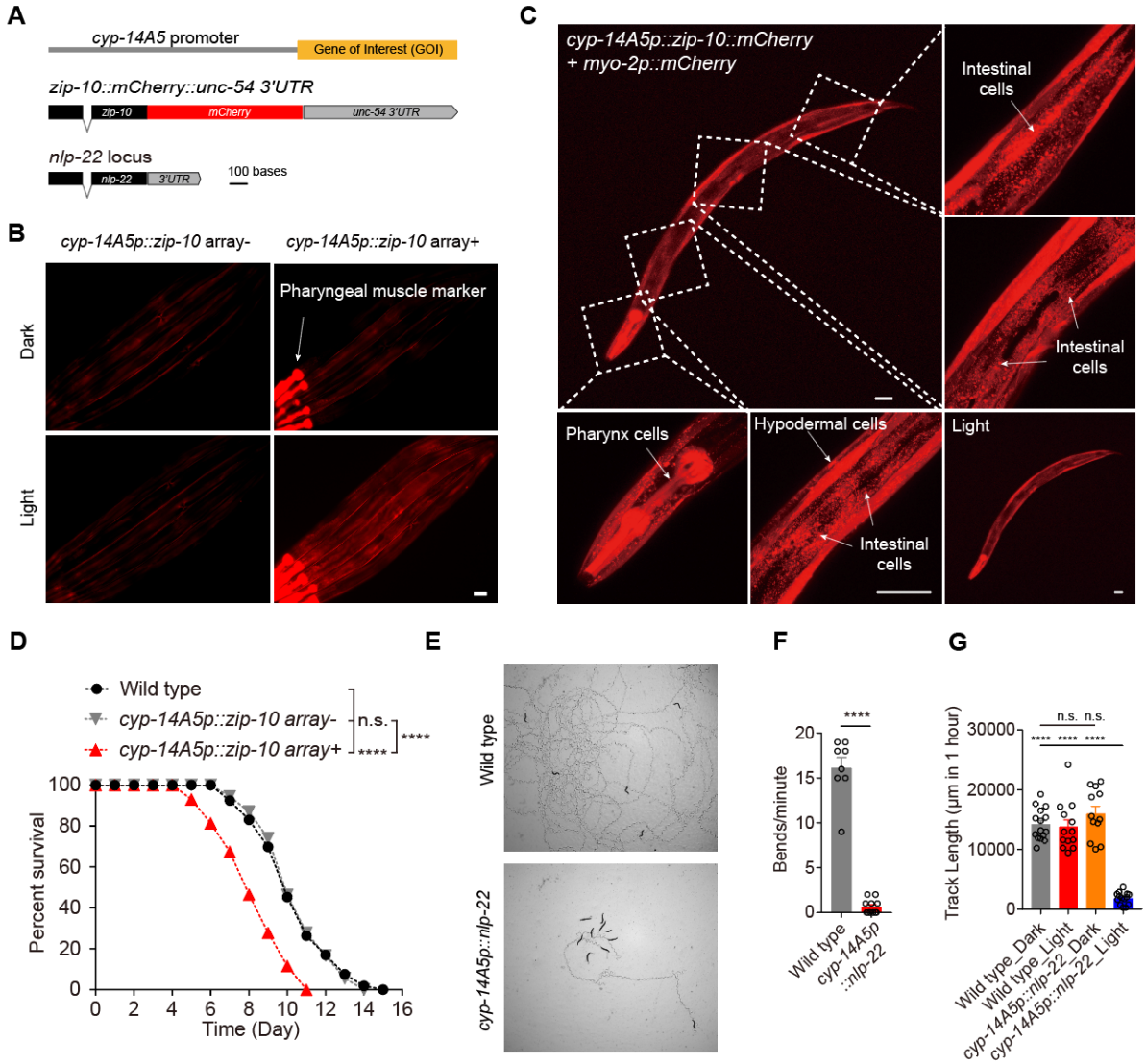


448

449 **Figure 4 Light-induced gene expression drives organismal phenotypes, including**

450 **sleep and shortened lifespans**. A, Schematic of synthetic constructs for light-inducible

451 *nlp-22* and *zip-10::mCherry* using the *cyp-14A5* promoter. B, Representative compound

452 epifluorescence images showing light-induced *cyp-14A5p::zip-10::mCherry* activation.
453 Scale bar: 50 μm. C, Representative confocal fluorescence images showing light-
454 induced *cyp-14A5p::zip-10::mCherry* activation (1500 Lux, 48 hrs starting at 24 hrs post
455 L4) in major non-neuronal tissues (hypoderm, intestinal cells indicated by arrows). Scale
456 bar: 50 μm. D, Representative lifespan curves showing that light-induced *zip-10* can
457 markedly shorten lifespan. **** indicates $P < 0.0001$. E, Representative bright field
458 images showing quiescent sleep behaviors by light-induced *cyp-14A5p::nlp-22*
459 expression. F, Quantification of population bending frequencies for light-treated (1500
460 Lux, 48 hrs starting at 24 hrs post L4) control wild type and *cyp-14A5p::nlp-22* animals.
461 G, Quantification of population track lengths for control wild type and *cyp-14A5p::nlp-22*
462 animals with light (1500 Lux, 48 hrs starting at 24 hrs post L4) or darkness treatments.
463 *** indicates $P < 0.001$, **** indicates $P < 0.0001$, n.s., non-significant.

464

465

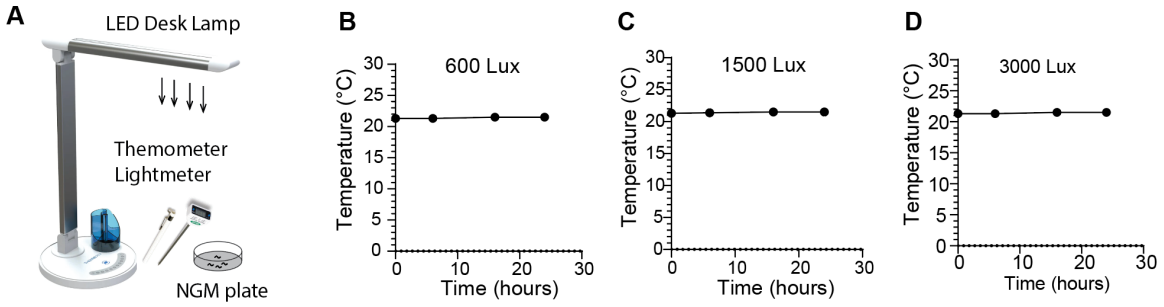


466

467 **Figure S1 Light for *cyp-14A5p::GFP* induction does not alter ambient**
468 **temperature.** A, Schematic of the setup for measurements of light intensity and
469 temperature at a plane (in parallel to LED light sources) where animals are exposed to

470 LED light in NGM plates. B, Measurements of temperature at the 600 Lux light intensity
471 showing no change of temperature over 24 hrs. C, Measurements of temperature at the
472 1500 Lux light intensity showing no change of temperature over 24 hrs. D,
473 Measurements of temperature at the 3000 Lux light intensity showing no change of
474 temperature over 24 hrs.

**A**

Gene ontology analysis
by WormCat:

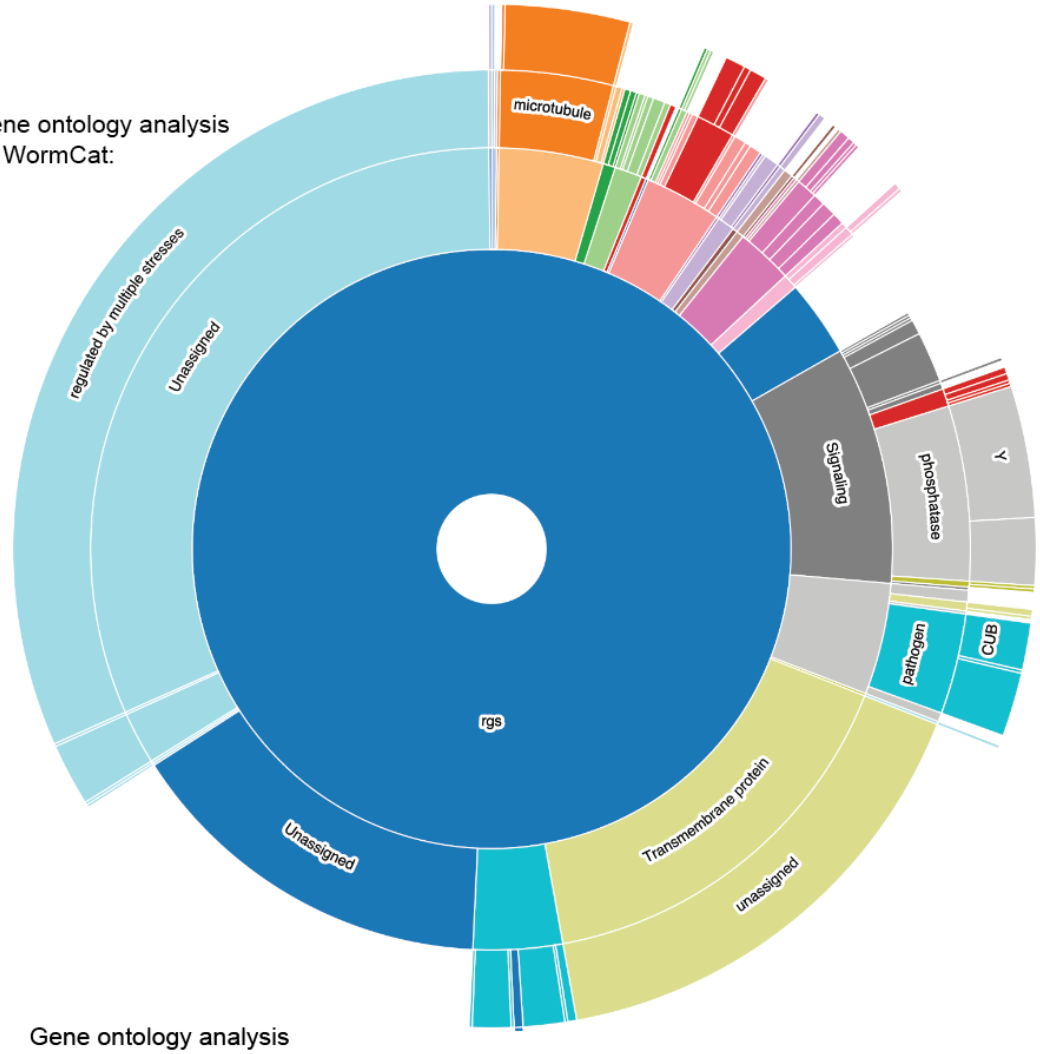


**B** Gene ontology analysis
by WormEnrichr:

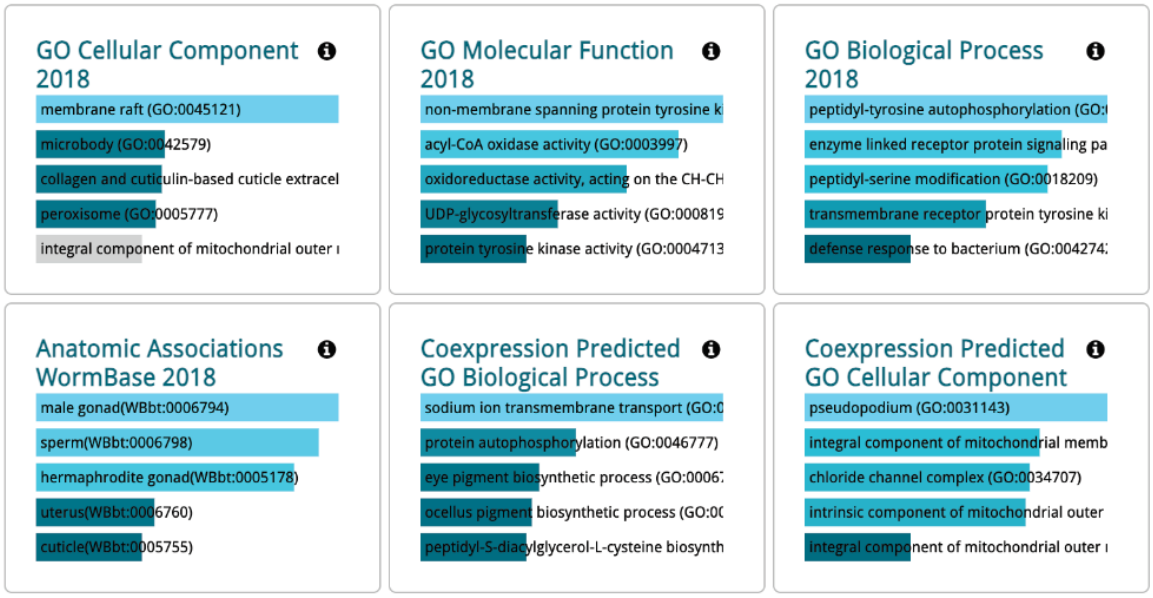


475

476 **Figure S2 Gene ontology analysis of light-induced transcriptomic changes.** A,
477 Starburst plot of gene ontology analysis of light-induced genes using WormCat
478 (http://www.wormcat.com/). B, Table summary of gene ontology analysis of light-
479 induced genes using WormEnrichr (https://maayanlab.cloud/WormEnrichr/).

480

481

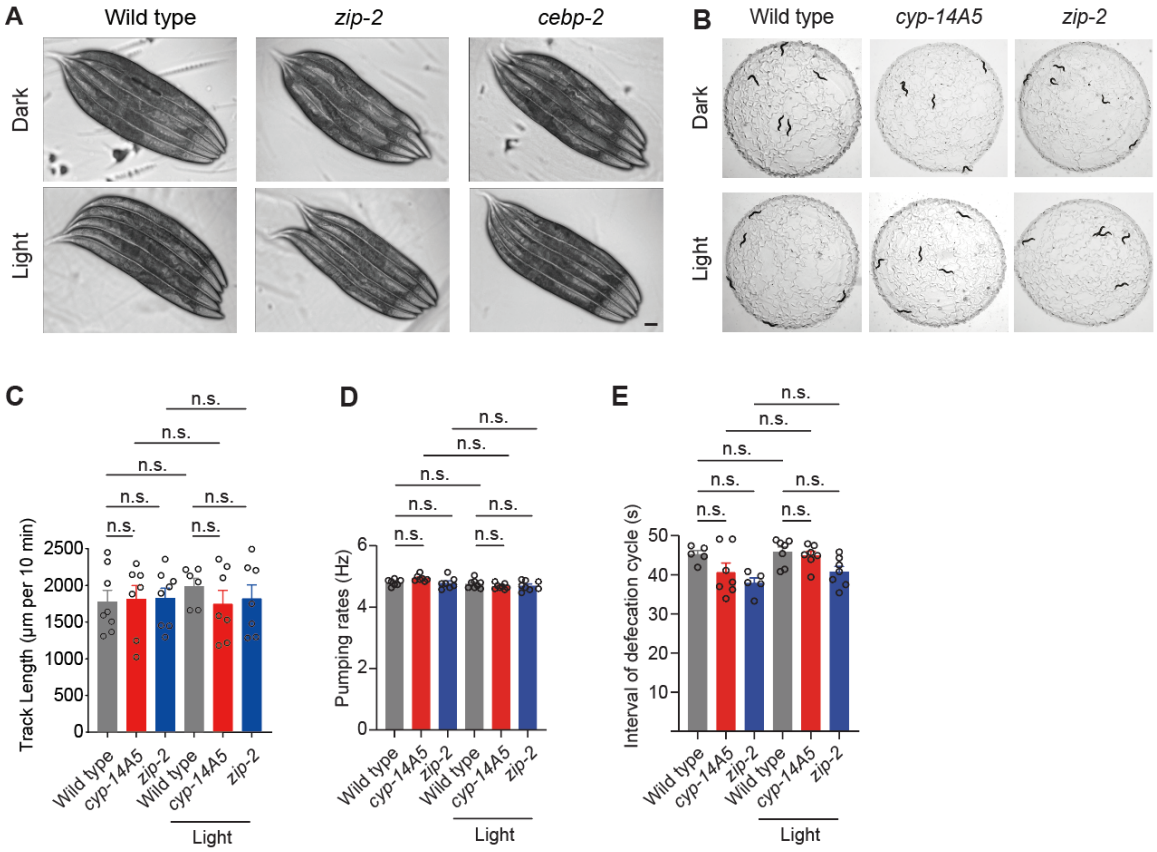


482

483 **Figure S3 No apparent effect of short-term visible light exposure on development,**
484 **morphology and simple behaviors.** A, Representative brightfield images showing no
485 apparent effects of visible light exposure (1500 Lux, 24 hrs) on the body lengths and
486 gross morphology of wild type, *cebp-2*, and *zip-2* loss-of-function mutants. Scale bar: 50

μm. B. Representative images showing the movement tracks of wild type, *cyp-14A5*, and *zip-2* loss-of-function mutants under dark and light (1500 Lux, 24 hrs) conditions. C, Quantification of track lengths of wild type, *cyp-14A5*, and *zip-2* loss-of-function mutants under dark and light (1500 Lux, 24 hrs) conditions. D, Quantification of pumping rates of wild type, *cyp-14A5*, and *zip-2* loss-of-function mutants under dark and light (1500 Lux, 24 hrs) conditions. E, Quantification of defecation behaviors of wild type, *cyp-14A5*, and *zip-2* loss-of-function mutants under dark and light (1500 Lux, 24 hrs) conditions.

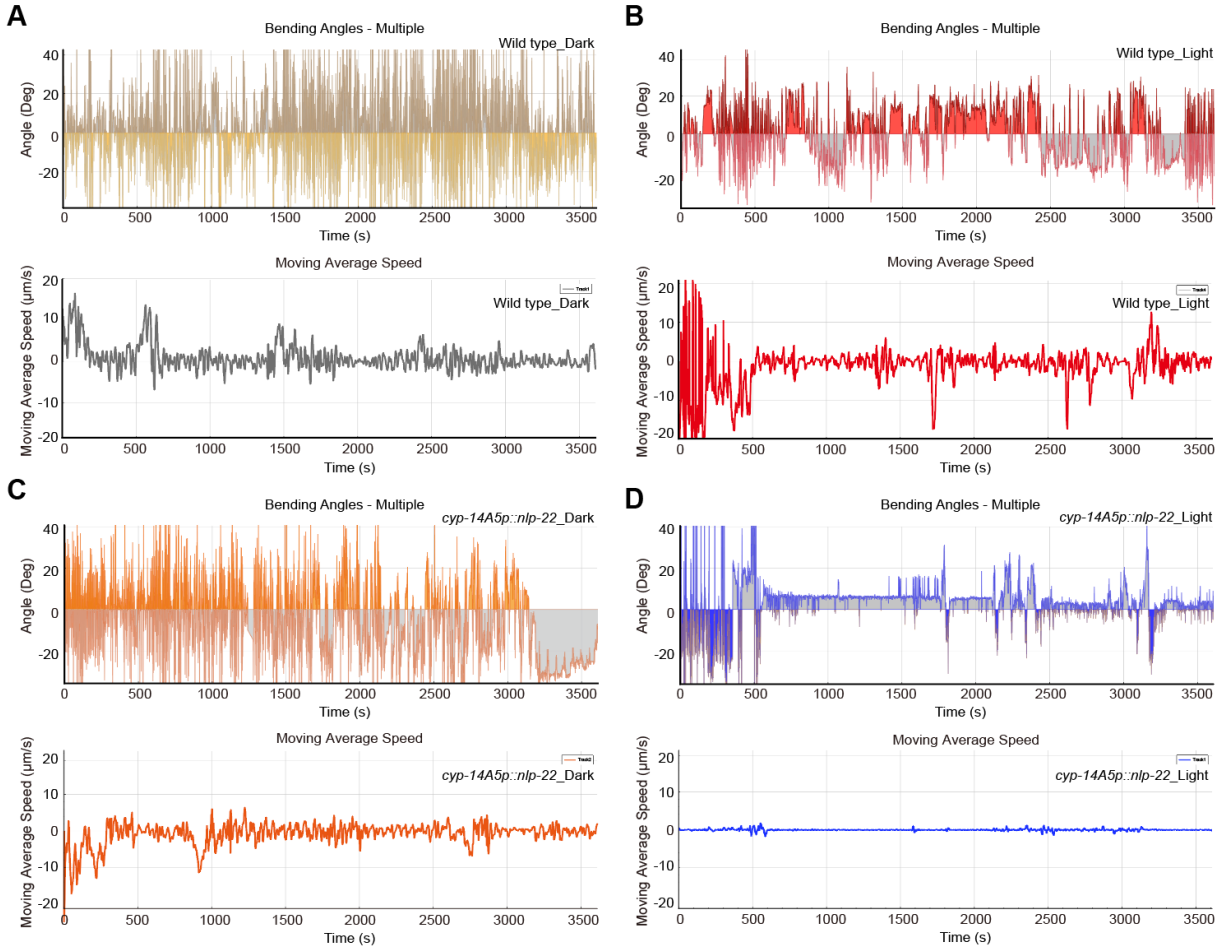

496 **Figure S4 WormLab analysis reveals sleep bouts caused by light-induced *cyp-*
497 ***14A5p::nlp-22* expression.** (A) Representative tracking of moving angles for body
498 posture and average speed for control animals under dark conditions (N=15). (B)
499 Representative tracking of moving angles for body posture and average speed for
500 control animals after light exposure conditions (1500 Lux, 24 hrs, N=13). (C)
501 Representative tracking of moving angles for body posture and average speed for *cyp-*
502 *14A5p::nlp-22* transgenic animals under dark conditions (N=12). (B) Representative
503 tracking of moving angles for body posture and average speed for *cyp-14A5p::nlp-22*
504 transgenic animals after light exposure conditions (1500 Lux, 24 hrs, N=13).

505

506

507 ## References


508 1. Andrabi, M., Upton, B.A., Lang, R.A., and Vemaraju, S. (2023). An Expanding Role for Nonvisual Opsins
509 in Extraocular Light Sensing Physiology. Annu Rev Vis Sci *9*, 245–267.
510 https://doi.org/10.1146/annurev-vision-100820-094018.

511 2. Cronin, T.W., and Johnsen, S. (2016). Extraocular, Non-Visual, and Simple Photoreceptors: An
512 Introduction to the Symposium. Integr Comp Biol *56*, 758–763. https://doi.org/10.1093/icb/icw106.

513 3. Van Gelder, R.N. (2008). Non-visual photoreception: sensing light without sight. Curr Biol *18*, R38-39.
514 https://doi.org/10.1016/j.cub.2007.11.027.

515 4. Do, M.T.H., and Yau, K.-W. (2010). Intrinsically photosensitive retinal ganglion cells. Physiol Rev *90*,
516 1547–1581. https://doi.org/10.1152/physrev.00013.2010.

517 5. Shi, Y., Zhang, J., Li, X., Han, Y., Guan, J., Li, Y., Shen, J., Tzvetanov, T., Yang, D., Luo, X., et al. (2024).
518 Non-image-forming photoreceptors improve visual orientation selectivity and image perception.
519 Neuron, S0896-6273(24)00840-7. https://doi.org/10.1016/j.neuron.2024.11.015.

520 6. Lucas, R.J., Hattar, S., Takao, M., Berson, D.M., Foster, R.G., and Yau, K.-W. (2003). Diminished
521 pupillary light reflex at high irradiances in melanopsin-knockout mice. Science *299*, 245–247.
522 https://doi.org/10.1126/science.1077293.

523 7. Berson, D.M., Dunn, F.A., and Takao, M. (2002). Phototransduction by retinal ganglion cells that set
524 the circadian clock. Science *295*, 1070–1073. https://doi.org/10.1126/science.1067262.

525 8. Hattar, S., Lucas, R.J., Mrosovsky, N., Thompson, S., Douglas, R.H., Hankins, M.W., Lem, J., Biel, M.,
526 Hofmann, F., Foster, R.G., et al. (2003). Melanopsin and rod-cone photoreceptive systems account for

527 all major accessory visual functions in mice. Nature *424*, 76–81.
528 https://doi.org/10.1038/nature01761.

529 9. Bhatla, N., and Horvitz, H.R. (2015). Light and hydrogen peroxide inhibit C. elegans Feeding through
530 gustatory receptor orthologs and pharyngeal neurons. Neuron *85*, 804–818.
531 https://doi.org/10.1016/j.neuron.2014.12.061.

532 10. Gong, J., Yuan, Y., Ward, A., Kang, L., Zhang, B., Wu, Z., Peng, J., Feng, Z., Liu, J., and Xu, X.Z.S.
533 (2016). The C. elegans Taste Receptor Homolog LITE-1 Is a Photoreceptor. Cell *167*, 1252-1263.e10.
534 https://doi.org/10.1016/j.cell.2016.10.053.

535 11. Hanson, S.M., Scholüke, J., Liewald, J., Sharma, R., Ruse, C., Engel, M., Schüler, C., Klaus, A.,
536 Arghittu, S., Baumbach, F., et al. (2023). Structure-function analysis suggests that the photoreceptor
537 LITE-1 is a light-activated ion channel. Curr Biol *33*, 3423-3435.e5.
538 https://doi.org/10.1016/j.cub.2023.07.008.

539 12. Edwards, S.L., Charlie, N.K., Milfort, M.C., Brown, B.S., Gravlin, C.N., Knecht, J.E., and Miller, K.G.
540 (2008). A novel molecular solution for ultraviolet light detection in Caenorhabditis elegans. PLoS Biol
541 *6*, e198. https://doi.org/10.1371/journal.pbio.0060198.

542 13. Bhatla, N., and Horvitz, H.R. (2015). Light and hydrogen peroxide inhibit C. elegans Feeding
543 through gustatory receptor orthologs and pharyngeal neurons. Neuron *85*, 804–818.
544 https://doi.org/10.1016/j.neuron.2014.12.061.

545 14. Mahmoud, B.H., Ruvolo, E., Hexsel, C.L., Liu, Y., Owen, M.R., Kollias, N., Lim, H.W., and Hamzavi,
546 I.H. (2010). Impact of long-wavelength UVA and visible light on melanocompetent skin. J Invest
547 Dermatol *130*, 2092–2097. https://doi.org/10.1038/jid.2010.95.

548 15. De Magalhaes Filho, C.D., Henriquez, B., Seah, N.E., Evans, R.M., Lapierre, L.R., and Dillin, A.
549 (2018). Visible light reduces C. elegans longevity. Nat Commun *9*, 927.
550 https://doi.org/10.1038/s41467-018-02934-5.

551 16. Liebel, F., Kaur, S., Ruvolo, E., Kollias, N., and Southall, M.D. (2012). Irradiation of skin with
552 visible light induces reactive oxygen species and matrix-degrading enzymes. J Invest Dermatol *132*,
553 1901–1907. https://doi.org/10.1038/jid.2011.476.

554 17. Keller, J., Ellieva, A., Ma, D.K., Ju, J., Nehk, E., Konkel, A., Falck, J.R., Schunck, W.-H., and Menzel,
555 R. (2014). CYP-13A12 of the nematode Caenorhabditis elegans is a PUFA-epoxygenase involved in
556 behavioural response to reoxygenation. Biochem. J. *464*, 61–71.
557 https://doi.org/10.1042/BJ20140848.

558 18. Ma, D.K., Rothe, M., Zheng, S., Bhatla, N., Pender, C.L., Menzel, R., and Horvitz, H.R. (2013).
559 Cytochrome P450 drives a HIF-regulated behavioral response to reoxygenation by C. elegans. Science
560 *341*, 554–558. https://doi.org/10.1126/science.1235753.

561 19. Denisov, I.G., Makris, T.M., Sligar, S.G., and Schlichting, I. (2005). Structure and chemistry of
562 cytochrome P450. Chem Rev *105*, 2253–2277. https://doi.org/10.1021/cr0307143.

563 20. Neve, E.P.A., and Ingelman-Sundberg, M. (2010). Cytochrome P450 proteins: retention and
564 distribution from the endoplasmic reticulum. Curr Opin Drug Discov Devel *13*, 78–85.

565 21. Ciccia, A., and Elledge, S.J. (2010). The DNA damage response: making it safe to play with knives.
566 Mol Cell *40*, 179–204. https://doi.org/10.1016/j.molcel.2010.09.019.

567 22. Schuch, A.P., Moreno, N.C., Schuch, N.J., Menck, C.F.M., and Garcia, C.C.M. (2017). Sunlight
568 damage to cellular DNA: Focus on oxidatively generated lesions. Free Radic Biol Med *107*, 110–124.
569 https://doi.org/10.1016/j.freeradbiomed.2017.01.029.

570 23. Estes, K.A., Dunbar, T.L., Powell, J.R., Ausubel, F.M., and Troemel, E.R. (2010). bZIP transcription
571 factor zip-2 mediates an early response to Pseudomonas aeruginosa infection in Caenorhabditis
572 elegans. Proc Natl Acad Sci U S A *107*, 2153–2158. https://doi.org/10.1073/pnas.0914643107.

573 24. Reddy, K.C., Dunbar, T.L., Nargund, A.M., Haynes, C.M., and Troemel, E.R. (2016). The C. elegans
574 CCAAT-Enhancer-Binding Protein Gamma Is Required for Surveillance Immunity. Cell Rep *14*, 1581–
575 1589. https://doi.org/10.1016/j.celrep.2016.01.055.

576 25. Dunbar, T.L., Yan, Z., Balla, K.M., Smelkinson, M.G., and Troemel, E.R. (2012). C. elegans detects
577 pathogen-induced translational inhibition to activate immune signaling. Cell Host Microbe *11*, 375–
578 386. https://doi.org/10.1016/j.chom.2012.02.008.

579 26. Ma, Z., Horrocks, J., Mir, D.A., Cox, M., Ruzga, M., Rollins, J., and Rogers, A.N. (2023). The
580 integrated stress response protects against ER stress but is not required for altered translation and
581 lifespan from dietary restriction in Caenorhabditis elegans. Front Cell Dev Biol *11*, 1263344.
582 https://doi.org/10.3389/fcell.2023.1263344.

583 27. Costa-Mattioli, M., and Walter, P. (2020). The integrated stress response: From mechanism to
584 disease. Science *368*, eaat5314. https://doi.org/10.1126/science.aat5314.

585 28. Brito Querido, J., Díaz-López, I., and Ramakrishnan, V. (2024). The molecular basis of translation
586 initiation and its regulation in eukaryotes. Nat Rev Mol Cell Biol *25*, 168–186.
587 https://doi.org/10.1038/s41580-023-00624-9.

588 29. Mir, D.A., Ma, Z., Horrocks, J., and Rogers, A. (2024). Stress-Induced Eukaryotic Translational
589 Regulatory Mechanisms. J Clin Med Sci *8*, 1000277.

590 30. Chandra, R., Farah, F., Muñoz-Lobato, F., Bokka, A., Benedetti, K.L., Brueggemann, C., Saifuddin,
591 M.F.A., Miller, J.M., Li, J., Chang, E., et al. (2023). Sleep is required to consolidate odor memory and
592 remodel olfactory synapses. Cell *186*, 2911-2928.e20. https://doi.org/10.1016/j.cell.2023.05.006.

593 31. Kauffman, A.L., Ashraf, J.M., Corces-Zimmerman, M.R., Landis, J.N., and Murphy, C.T. (2010).
594 Insulin signaling and dietary restriction differentially influence the decline of learning and memory
595 with age. PLoS Biol *8*, e1000372. https://doi.org/10.1371/journal.pbio.1000372.

596 32. Wang, C., Long, Y., Wang, B., Zhang, C., and Ma, D.K. (2023). GPCR signaling regulates severe
597 stress-induced organismic death in Caenorhabditis elegans. Aging Cell *22*, e13735.
598 https://doi.org/10.1111/acel.13735.

599 33. Pandey, T., and Ma, D.K. (2022). Stress-Induced Phenoptosis: Mechanistic Insights and
600 Evolutionary Implications. Biochemistry (Mosc) *87*, 1504–1511.
601 https://doi.org/10.1134/S0006297922120082.

602 34. Bringmann, H. (2018). Sleep-Active Neurons: Conserved Motors of Sleep. Genetics *208*, 1279–
603 1289. https://doi.org/10.1534/genetics.117.300521.

604 35. Van der Auwera, P., Frooninckx, L., Buscemi, K., Vance, R.T., Watteyne, J., Mirabeau, O.,
605 Temmerman, L., De Haes, W., Fancsalszky, L., Gottschalk, A., et al. (2020). RPamide neuropeptides
606 NLP-22 and NLP-2 act through GnRH-like receptors to promote sleep and wakefulness in C. elegans.
607 Sci Rep *10*, 9929. https://doi.org/10.1038/s41598-020-66536-2.

608 36. Nelson, M.D., Trojanowski, N.F., George-Raizen, J.B., Smith, C.J., Yu, C.-C., Fang-Yen, C., and
609 Raizen, D.M. (2013). The neuropeptide NLP-22 regulates a sleep-like state in Caenorhabditis elegans.
610 Nat Commun *4*, 2846. https://doi.org/10.1038/ncomms3846.

611 37. Troemel, E.R., Chu, S.W., Reinke, V., Lee, S.S., Ausubel, F.M., and Kim, D.H. (2006). p38 MAPK
612 regulates expression of immune response genes and contributes to longevity in C. elegans. PLoS
613 Genet *2*, e183. https://doi.org/10.1371/journal.pgen.0020183.

614 38. Wong, D., Bazopoulou, D., Pujol, N., Tavernarakis, N., and Ewbank, J.J. (2007). Genome-wide
615 investigation reveals pathogen-specific and shared signatures in the response of Caenorhabditis
616 elegans to infection. Genome Biol *8*, R194. https://doi.org/10.1186/gb-2007-8-9-r194.

617 39. Sinha, A., Rae, R., Iatsenko, I., and Sommer, R.J. (2012). System wide analysis of the evolution of
618 innate immunity in the nematode model species Caenorhabditis elegans and Pristionchus pacificus.
619 PLoS One *7*, e44255. https://doi.org/10.1371/journal.pone.0044255.

620 40. Genuth, N.R., and Barna, M. (2018). Heterogeneity and specialized functions of translation
621 machinery: from genes to organisms. Nat Rev Genet *19*, 431–452. https://doi.org/10.1038/s41576-
622 018-0008-z.

623 41. D'Orazio, K.N., and Green, R. (2021). Ribosome states signal RNA quality control. Mol Cell *81*,
624 1372–1383. https://doi.org/10.1016/j.molcel.2021.02.022.

625 42. Sinha, N.K., McKenney, C., Yeow, Z.Y., Li, J.J., Nam, K.H., Yaron-Barir, T.M., Johnson, J.L.,
626 Huntsman, E.M., Cantley, L.C., Ordureau, A., et al. (2024). The ribotoxic stress response drives UV-
627 mediated cell death. Cell *187*, 3652-3670.e40. https://doi.org/10.1016/j.cell.2024.05.018.

628 43. Zhang, B., Gong, J., Zhang, W., Xiao, R., Liu, J., and Xu, X.Z.S. (2018). Brain-gut communications
629 via distinct neuroendocrine signals bidirectionally regulate longevity in C. elegans. Genes Dev *32*,
630 258–270. https://doi.org/10.1101/gad.309625.117.

631 44. Fukuda, A., Sato, K., Fujimori, C., Yamashita, T., Takeuchi, A., Ohuchi, H., Umatani, C., and Kanda,
632 S. (2025). Direct photoreception by pituitary endocrine cells regulates hormone release and
633 pigmentation. Science *387*, 43–48. https://doi.org/10.1126/science.adj9687.

634 45. Liu, Y., Zhou, J., Zhang, N., Wu, X., Zhang, Q., Zhang, W., Li, X., and Tian, Y. (2022). Two sensory
635 neurons coordinate the systemic mitochondrial stress response via GPCR signaling in C. elegans. Dev
636 Cell *57*, 2469-2482.e5. https://doi.org/10.1016/j.devcel.2022.10.001.

637 46. Aghayeva, U., Bhattacharya, A., Sural, S., Jaeger, E., Churgin, M., Fang-Yen, C., and Hobert, O.
638 (2021). DAF-16/FoxO and DAF-12/VDR control cellular plasticity both cell-autonomously and via
639 interorgan signaling. PLoS Biol *19*, e3001204. https://doi.org/10.1371/journal.pbio.3001204.

640 47. Stringham, E.G., Dixon, D.K., Jones, D., and Candido, E.P. (1992). Temporal and spatial
641 expression patterns of the small heat shock (hsp16) genes in transgenic Caenorhabditis elegans. Mol
642 Biol Cell *3*, 221–233. https://doi.org/10.1091/mbc.3.2.221.

643 48. Monsalve, G.C., Yamamoto, K.R., and Ward, J.D. (2019). A New Tool for Inducible Gene
644 Expression in Caenorhabditis elegans. Genetics *211*, 419–430.
645 https://doi.org/10.1534/genetics.118.301705.

646 49. Wei, X., Potter, C.J., Luo, L., and Shen, K. (2012). Controlling gene expression with the Q
647 repressible binary expression system in Caenorhabditis elegans. Nat Methods *9*, 391–395.
648 https://doi.org/10.1038/nmeth.1929.

649 50. Brenner, S. (1974). The genetics of Caenorhabditis elegans. Genetics *77*, 71–94.

650 51. Hobert, O. (2002). PCR fusion-based approach to create reporter gene constructs for expression
651 analysis in transgenic C. elegans. Biotechniques *32*, 728–730. https://doi.org/10.2144/02324bm01.

652 52. Liao, Y., Smyth, G.K., and Shi, W. (2014). featureCounts: an efficient general purpose program
653 for assigning sequence reads to genomic features. Bioinformatics *30*, 923–930.
654 https://doi.org/10.1093/bioinformatics/btt656.

655 53. Kim, D., Langmead, B., and Salzberg, S.L. (2015). HISAT: a fast spliced aligner with low memory
656 requirements. Nat. Methods *12*, 357–360. https://doi.org/10.1038/nmeth.3317.

657 54. Love, M.I., Huber, W., and Anders, S. (2014). Moderated estimation of fold change and
658 dispersion for RNA-seq data with DESeq2. Genome Biol. *15*, 550. https://doi.org/10.1186/s13059-
659 014-0550-8.

660